



Generic identification and classification of morphostructures in the Noachis-Sabaea region, southern highlands of Mars

Trishit Ruj, Goro Komatsu, James M. Dohm, Hirdy Miyamoto & Francesco Salese

To cite this article: Trishit Ruj, Goro Komatsu, James M. Dohm, Hirdy Miyamoto & Francesco Salese (2017) Generic identification and classification of morphostructures in the Noachis-Sabaea region, southern highlands of Mars, Journal of Maps, 13:2, 755-766, DOI: [10.1080/17445647.2017.1379913](https://doi.org/10.1080/17445647.2017.1379913)

To link to this article: <http://dx.doi.org/10.1080/17445647.2017.1379913>



© 2017 The Author(s). Published by Informa UK Limited, trading as Taylor & Francis Group on behalf of Journal of Maps



[View supplementary material](#)



Published online: 04 Oct 2017.



[Submit your article to this journal](#)








[View related articles](#)



[View Crossmark data](#)



Generic identification and classification of morphostructures in the Noachis-Sabaea region, southern highlands of Mars

Trishit Ruj ^{a,b}, Goro Komatsu ^{a,b}, James M. Dohm ^{c*}, Hirdy Miyamoto ^c and Francesco Salese ^{a,d}

^aInternational Research School of Planetary Sciences, Università d'Annunzio, Pescara, Italy; ^bDipartimento di Ingegneria e Geologia, Università degli Studi G. d'Annunzio, Chieti, Pescara, Italy; ^cThe University Museum, University of Tokyo, Tokyo, Japan; ^dExploration and Observation of the Universe Department, Italian Space Agency (ASI), Rome, Italy

ABSTRACT

The Noachis-Sabaea region in the southern highlands preserves some of the oldest Martian crust. It records deformation by both endogenic and exogenic processes. This deformation includes giant impacts and their impact stresses, which could have resulted in both the reactivation and modification of pre-impact tectonic structures, in addition to impact-generated tectonic structures. There are also widespread extensional and compressional tectonic structures, which were formed due to endogenic processes. We have produced the first detailed morphostructural map of the Noachis-Sabaea region, which details the characteristics and spatial arrangements of structures in the region, forms the basis for making inferences about Noachian-Hesperian crustal activity, and provides information for further studies regarding the reconstruction of the evolutionary history of the region.

ARTICLE HISTORY

Received 9 March 2017
Revised 7 August 2017
Accepted 12 September 2017

KEYWORDS


Noachis-sabaea; Hellas grabens; morphostructural analysis; Hellas impact stress

1. Introduction

Mars is, after Earth, the planet most studied from global to local scales. Mars has been mapped globally earlier by Scott and Carr (1978) at a scale of 1:25,000,000 using 1–2 km/pixel to more recently by Tanaka, Robbins, Fortezzo, Skinner, and Hare (2014) at a 1:20,000,000 scale, using high-resolution data up to 6 m/pixel. The majority of morphostructural studies have been focused on Tharsis and its components. Both flexural-loading stresses (e.g. Anguita et al., 2001; Banerdt, Golombek, & Tanaka, 1992; Carr, 1981; Davis, Tanaka, & Golombek, 1995; Mège & Masson, 1996) and magmatic-driven uplift and subsidence (Anderson et al., 2001; Dohm et al., 2001; Lowry & Zhong, 2003) may explain the type, location, orientation, and strain of most tectonic features in and around Tharsis. Less attention has been paid to the more ancient terrains of the southern highlands in part due to the limited coverage of high-resolution data and their highly degraded appearance. In the southern highlands, highly cratered and degraded early Noachian crust is preserved. On Earth, both dense basaltic oceanic crust and lighter felsic continental crust have formed through time, resulting in bimodal topography, with the continental crust generally being older and felsic in large part due to granite accumulating at subduction zones associated with the formation of orogenic complexes. In other cases, there is no plate tectonics to influence

crustal formation and composition, such as the Moon where the crust is generally composed of anorthosite-enriched highlands and basaltic lunar maria. In Mars, its bimodal topography raises question about the crustal modification through internal driven processes. With this in mind, the primary aim of our study is to help address this question through geological mapping investigation of the tectonic structures that occur in ancient terrains of Mars dating back more than 4.0 Ga. Here, we discuss the results of our mapping investigation (Main Map) which focuses on such ancient terrain of Mars with distinct systems of tectonic structures that includes the eastern part of Noachis Terra, the southern part of Terra Sabaea, and the northwest part of the giant Hellas impact structure, referred to here as the Noachis-Sabaea region (Figure 1).

The Hellas basin and surroundings, which include the Noachis-Sabaea region, have been studied with varying foci, including: crater degradation (Mangold, Adeli, Conway, Ansan, & Langlais, 2012), crater morphology (Öhman, Aittola, Kostama, & Raitala, 2005), magmatic activity such as at Tyrrhenus and Hadriacus Montes (Crown & Greeley, 1993; Head, Kreslavsky, & Pratt, 2002), anomalous features (including magnetic and gravity signatures, and elemental enrichment) in Arabia Terra (Dohm et al., 2007), valleys/channels and sedimentary

CONTACT Trishit Ruj  trishit@irsps.unich.it  Research Student, International Research School of Planetary Sciences, Università d'Annunzio, Viale Pindaro, 42, Pescara 65127, Italy

*Current address: Foundation for Advancement of International Science, 24-16, Kasuga, 3-chome, Tsukuba, Ibaraki 305-0821, Japan

© 2017 The Author(s). Published by Informa UK Limited, trading as Taylor & Francis Group on behalf of Journal of Maps

This is an Open Access article distributed under the terms of the Creative Commons Attribution License (<http://creativecommons.org/licenses/by/4.0/>), which permits unrestricted use, distribution, and reproduction in any medium, provided the original work is properly cited.

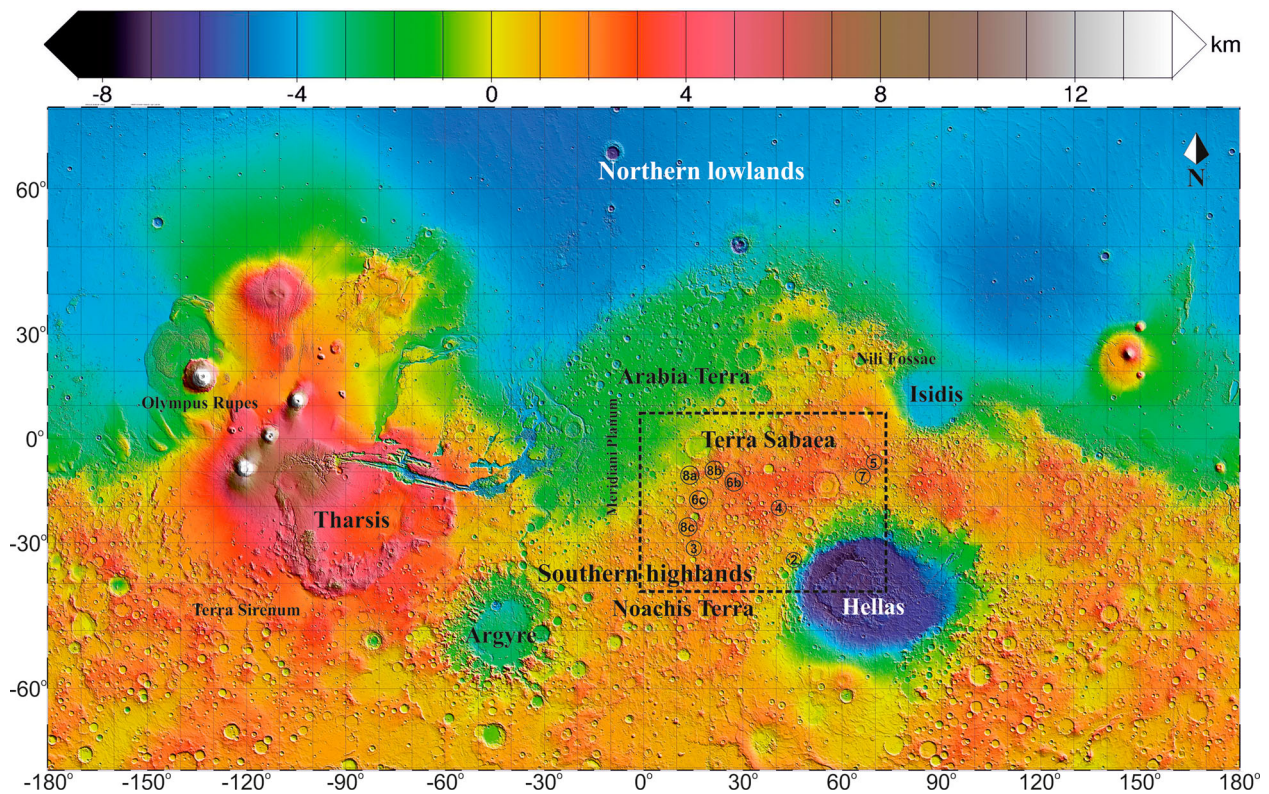


Figure 1. MOLA colourised elevation map. Study area (Noachis-Sabaea region) is shown in the dotted black rectangle. Also the locations are shown of Figures 2–8 (solid circle with corresponding number).

processes (Buczowski et al., 2010; Davis, Balme, Grindrod, Williams, & Gupta, 2016), and the possible presence of episodic methane releases (Mumma et al., 2009). However, there is no detailed geological mapping investigation of the Noachis-Sabaea region with a particular focus on the ancient tectonic structures and their formational histories, except for some specific investigations such as radial dike structures and some ridges near Hellas (Head et al., 2002; Wilson & Head, 2002). An investigation of the paleotectonic history of Mars, based on Viking data, indicated several centres of tectonism in the eastern hemisphere (Anderson et al., 2008).

Extensional (grabens, rifts, troughs) and compressional structures (wrinkle ridges (WR), lobate scarps) are common on Mars (e.g. Anguita et al., 1997; Sleep, 1994; Watters, 1993). While the responsible stresses are sometimes mentioned to be related to mega impacts such as Hellas, Isidis, and Argyre (Frey & Schultz, 1988; Wilhelms & Squyres, 1984; Yin, 2012), endogenic processes have played a key role in the paleotectonic evolution of Mars. Endogenic activity may have included mobile lithospheric activity including some form of plate tectonic activity involving both extension and subduction (Baker, Maruyama, & Dohm, 2007; Sleep, 1994). An ancient phase of plate tectonics has also been proposed to explain magnetic anomalies among other features in the southern highlands (Connerney et al., 1999, 2005; Dohm et al., 2002, 2016; Fairén, Ruiz, & Anguita, 2002; Fairén & Dohm, 2004).

In order to study the ancient Martian crustal basement in the southern highlands and its recorded tectonic history, including both impact and endogenic-induced structures, our primary objective was to produce a detailed map delineating the spatial arrangement of the various morphostructural types. In this work, we present our geological map of the Noachis-Sabaea region that includes discussion of the morphostructural elements and their classification, as well as interpretation of their origins including associated stress regimes.

2. Geological setting

The Noachis-Sabaea region (Figure 1) preserves some of the oldest highland terrains of Mars (Leonard & Tanaka, 2001; Tanaka & Leonard, 1995). The study region is bordered by the Hellas basin to the southeast, the Isidis basin to the northeast, Arabia Terra and dichotomy boundary to the north, the Argyre basin to the south-west (Greeley & Guest, 1987; Scott & Carr, 1978), and Meridiani Planum to the northwest. Impact cratering has erased some of the small-scale structures. The observed modern-day surface also records volcanic, fluvial, aeolian, mass wasting. The distribution of fluvial channels is more concentrated in the northern and central parts of the study area.

Rogers, Bandfield, and Christensen (2007) characterised most of the study area to be relatively low in feldspar content, low in Ca-pyroxene content, and relatively high in olivine content (they refer to as ‘group 3’) based on the

analysis of Thermal Emission Spectrometer (TES) data, which they interpret to be a typical Noachian highland unit (i.e. heavily influenced and reshaped by giant impacts). The mega impacts not only influenced the earlier endogenic structures but also have produced relatively thick ejecta and basin-concentric grabens (Peterson, 1977; Rogers & Nazarian, 2013) due to impact-related stress relaxation (Melosh, 1976; Melosh & McKinnon, 1978). Spectroscopic analyses of parts of the Noachis-Sabaea region using the Compact Reconnaissance Imaging Spectrometer for Mars (CRISM) data have revealed spectral features interpreted to be flood basalts of Noachian age (Rogers & Nazarian, 2013) and feldspathic rocks including possible granite to the northwest of the Hellas basin (Wray et al., 2013). The northeastern to central part of the study region is dominated by flood basalts from the Syrtis Major volcanic province, deformed mainly by WR. WR occur both within and outside impact crater basins and have a more or less consistent NNW-SSE orientation.

Local occurrences of sedimentary rocks have been reported for the outer margin of the Hellas basin (Ansan et al., 2011; Salese et al., 2016). WR in the Noachis-Sabaea region are found on the floor of Noachian-Hesperian units. Some of these materials could be flood basalts, consistent with global Martian flood volcanism proposed to have occurred during the Hesperian Period (Carr & Head, 2010). Wrinkle ridge (Watters, 1993) formation and sedimentary processes of inter crater plains (Salese et al., 2016), along with magmatism and associated outflow channel activity (Fairén et al., 2003; Komatsu, Dohm, & Hare, 2004, and references therein), are key processes in the Hesperian.

Linear ridges are interpreted to result from a high effusion rate of volcanism (Head, Wilson, Dickson, & Neukum, 2006). These ridges are often observed to transect Hesperian units. The origin of these linear ridges are interpreted to be igneous dikes, caused by the propagation of magma-filled fractures in the crust; the magma eventually solidifies and becomes exposed at the Martian surface as a long ridge due to differential erosion of the more competent solidified magma and more friable surrounding sediments.

In and nearby our study region, Amazonian geology may include sedimentary deposits and dust, as interpreted for the Hellas basin (Ormö & Komatsu, 2003), as well as glacial features (e.g. glacial scouring, fluted moraine, cryoturbation patterns, and iceberg plow marks) and dunes along the floors of impact craters.

3. Data and geological mapping process

3.1. Data

Mars Express High Resolution Stereoscopic Camera (HRSC) nadir images (Jaumann et al., 2007; Neukum & Jaumann, 2004), with a resolution of ~ 12.5 m/

pixel, enabled geological mapping from a morphologic point of view. We mainly used HRSC (Levels 4 and 3) images as a base in which to map the tectonic features in the Noachis-Sabaea region. Based on Mars Orbiter Laser Altimeter (MOLA) data, geometrically corrected Level 3 HRSC images cover almost entire Martian surface, whereas, the new Digital Terrain Model (DTMs) and ortho-images are Level-4 data products of the HRSC. Level 4 HRSC images cover 12% of the surface. The Context (CTX) camera images (average image resolution of 6 m/pixel) (Malin et al., 2007) provided detailed observations of features such as tectonic structures. We used CTX images and Thermal Emission Imaging System (THEMIS) daytime (Ruff & Christensen, 2002) IR mosaic images; in particular, CTX was used to fill in the areas void of HRSC data. Mapping was performed combining image data along with altimetry data at different scales like Mars Orbiter Laser Altimeter (MOLA) (Smith et al., 1999) at ~ 463 m/pixel, and where available, Digital Elevation Models (DEM) made from HRSC stereo images at ~ 12.5 –50 m/pixel.

4. Mapping method and morphostructural analysis

We have produced a morphostructural map of the Noachis-Sabaea region at a scale of 1:5,000,000 following the USGS guideline for planetary mapping (Tanaka, Skinner, & Hare, 2009). The same coordinate system (GCS_Mars_2000_Sphere) used in producing the new global geological map by Tanaka et al. (2014) was used in the production of our map. Kilometer-long structures and impact craters were identified and mapped using THEMIS-IR daytime and nighttime images. The structures were then investigated in detail using HRSC images and CTX images. MOLA DEMs along with HRSC DTMs were useful for identifying structures through their derived profile sections.

Orientation-analysis to measure the distribution of the WR over the Noachis-Sabaea region was performed. This was done by fitting a best fitted-straight line following the trend of the wrinkle ridge and measuring the trend of the straight line. Rose diagram was used to analyse the trend.

Extensional features are formed when the maximum principle stress (σ_1) is vertical, the minimum principle stress (σ_3) is perpendicular, and the intermediate stress axis (σ_2) follows the strike of the extensional feature (Anderson, 1951). In this case, both σ_2 and σ_3 are horizontal. In case of a compressional feature, the maximum principle stress (σ_1) is horizontal and perpendicular to the strike of the compressional feature, σ_3 is vertical and σ_2 is horizontal and parallel to the structure (Anderson, 1951).

5. Description of the main elements of the morphostructural map

Extensional structures in the Noachis-Sabaea region are mapped and interpreted as half grabens bounded by basin-concentric normal faults produced by the Hellas and Isidis impacts. However, we also identified and mapped a series of faults (mapped as Set-2 and Set-3 grabens discussed below) that are neither concentric to nor radial about any of the giant impact basins such as Hellas, including those (Set-2) that have similar orientations of two parallel structures mapped and interpreted by Connerney et al. (2005) to indicate plate tectonics. These may have thus involved ancient endogenic-driven activity including a mobile lithosphere. Each structure type is described below.

5.1. Grabens

Grabens are distributed throughout our study region with varying widths up to 100 km. The grabens have different orientations implying varying stresses and modes of origin through time. These grabens have been classified on the basis of their orientations, morphology, and cross-cutting and stratigraphic relations among rock materials and structures including impact craters, namely sets 1, 2, and 3 (Ruj, Komatsu, Dohm, Miyamoto, & Salese, 2015, 2016).

5.1.1. Set-1 grabens

Set-1 grabens are concentric to the Hellas basin and concentrated along and in close proximity to the west-northwestern margin. They generally have

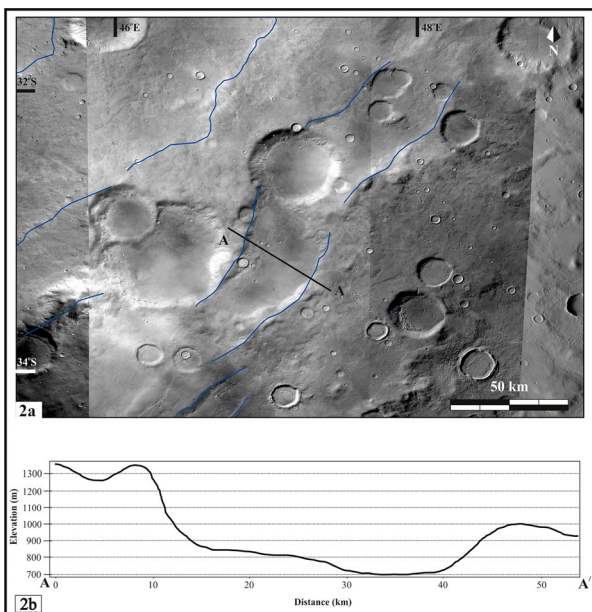


Figure 2. (a) HRSC images show the set-1 graben in the western flank of the Hellas basin. Transect A-A' is also shown of corresponding topographic profile in (b). (b) Topographic profile of a flat floored set-1 graben shown in (a).

the smallest dimensions of the three mapped graben sets, with an average width of 35 km and maximum length reaching 200 km. They are interpreted to have formed due to the Hellas impact. Our interpretation is consistent with that of Melosh (1976), who described grabens generated by impact-related stress relaxation. In addition, Wichman and Schultz (1989) reported that some of these grabens are Hellas impact-induced, near-basin concentric canyons circular to the giant impact basin. These grabens are well defined with flat floors, and their western walls occur at higher elevations than their eastern walls (Figure 2 (a,b)).

5.1.2. Set-2 grabens

Set-2 grabens are wider and greater in length than the Set-1 grabens. The longest graben is around 1200 km (Figure 3(a,b)), attaining a maximum width of 100 km. In the northern part of the longest graben, WR are observed along its floor possibly indicating volcanic rock materials. The orientations of these grabens trend to the northeast, antithetic to the Set-1 grabens that are generally concentric about the Hellas basin.

5.1.3. Set-3 grabens

A series of grabens form a linear trend that continues for nearly 1500 km. In general, they have a trend of east–west, but the trends of the individual grabens vary from east–west to northeast–southwest. Individual grabens are 40–50 km in width (Figure 4(a,b)). Some of the grabens are arcuate in shape, and some crosscut the southwest part of the Huygens crater. WR are not observed to the south of these Set-3 grabens. This set of grabens do not follow the outer arc curvature like as do the Hellas-concentric Set-1 grabens.

5.2. Normal faults

Either side of the normal faults show prominent elevation wise offset blocks (namely hangingwall and footwall block). These elevation offsets are observed through the extracted profile sections and the traces are mapped in this region. They are distributed on the northern part of the Set-3 grabens. There are two identified sets of normal faults in this region. One set is concentric about the Hellas basin, and the other concentric about the Isidis impact basin (Figure 5(a)). These faults could be due to crater-forming impact events, though some could be the result of activity that resulted in the formation of Set-2 grabens.

5.3. Wrinkle ridges

WR, interpreted to result from compressional stresses including those associated with the formation of

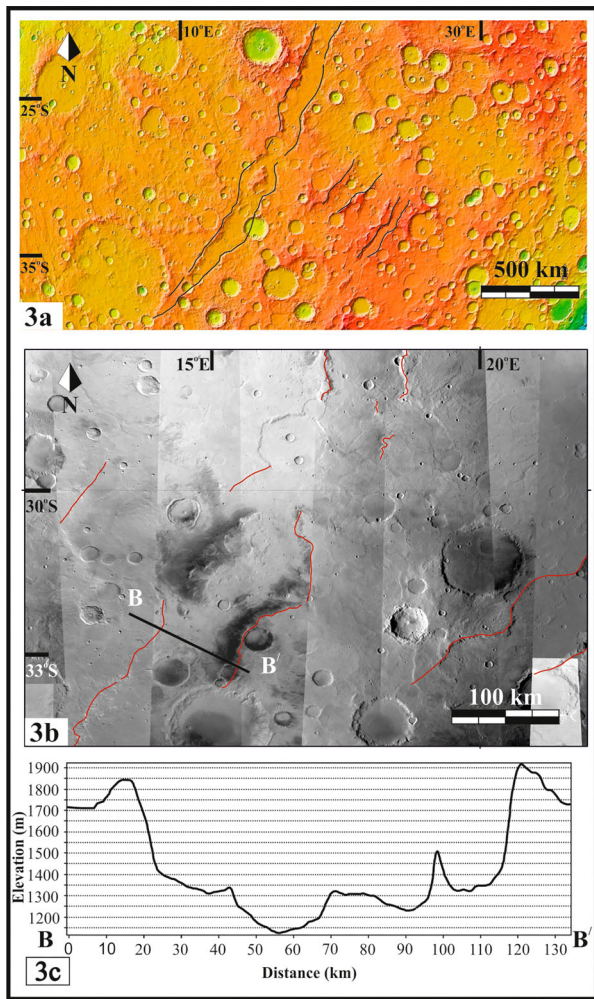


Figure 3. (a) Set-2 graben shown on the MOLA coloured elevation map (graben boundaries indicated by black lines). (b) Set-2 graben (boundaries indicated by red lines) mapped on HRSC image mosaic. Also shown is transect B-B' of corresponding topographic profile in (c). (c) Topographic profile across a graben shown in (b), displaying a typical extensional graben floor.

thrust faults and folds (Banerdt et al., 1992; Mangold, Allemand, & Thomas, 1998; Watters, 1993), are mapped both within (i.e. on the floors) and outside of the impact craters. Head et al. (2002) proposed that many WR formed in the upper crust as a result of global Martian Hesperian volcanic activity. The mapped WR in our map region have a NNW-SSE trend (Figure 6(a)), with spacing of 15–40 km. The trends of the WR are relatively consistent across the Noachis-Sabaea region. WR are limited in number to the south of the Set-3 grabens when compared to other parts of the Noachis-Sabaea map region, including along the northern and western margins of the Hellas basin. This could indicate compositional variation from north to south, or possible competency of the bedrock. The WR within the crater floor (Figure 6(b,c)) are shown differently in the map because of their unclear relationships to the regional stress field. Some WR are interpreted to be related to impact-induced volcanism and cooling within

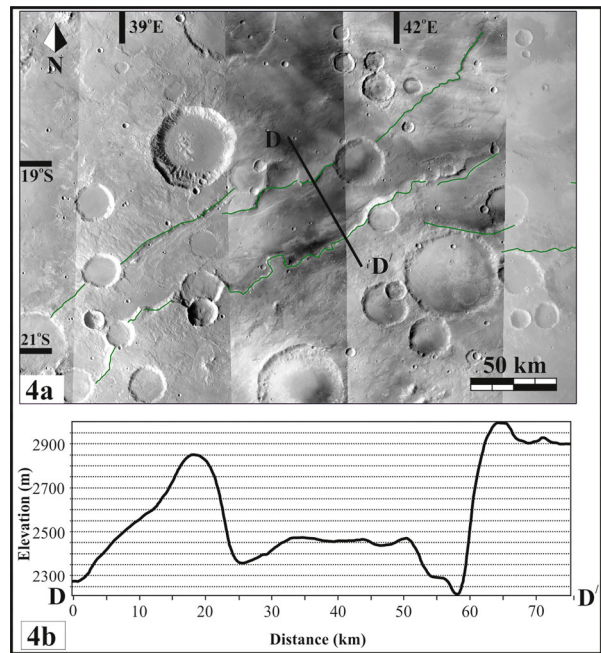


Figure 4. (a) Set-3 graben (graben boundaries indicated by green lines) and transect D-D' of corresponding topographic profile in (b) are shown.

crater floors in an isotropic condition. WR near the Syrtis Major volcanic province are also distributed centrally and radially with respect to the volcanic province.

5.4. Linear ridges/dikes

Parallel linear ridges have been identified and mapped in the Noachis-Sabaea region area (Figure 7), in some cases having lengths reaching 750 km (Wilson &

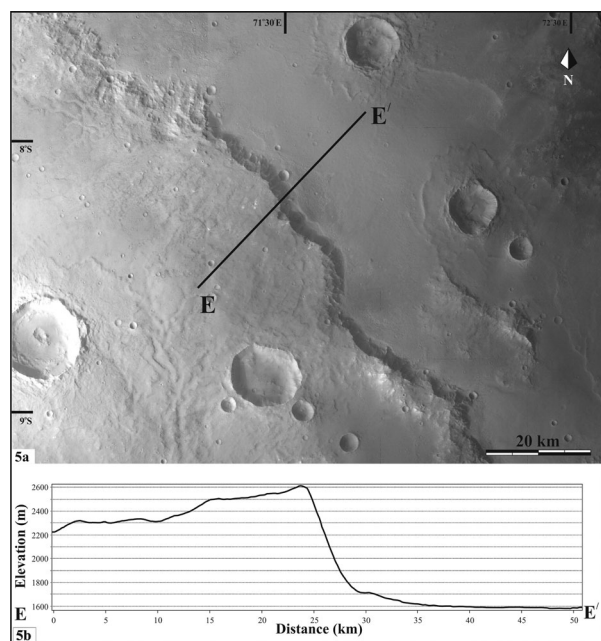


Figure 5. (a) HRSC image showing normal fault, centred about the Isidis basin. Also shown is transect E-E' with corresponding topographic profile in (b).

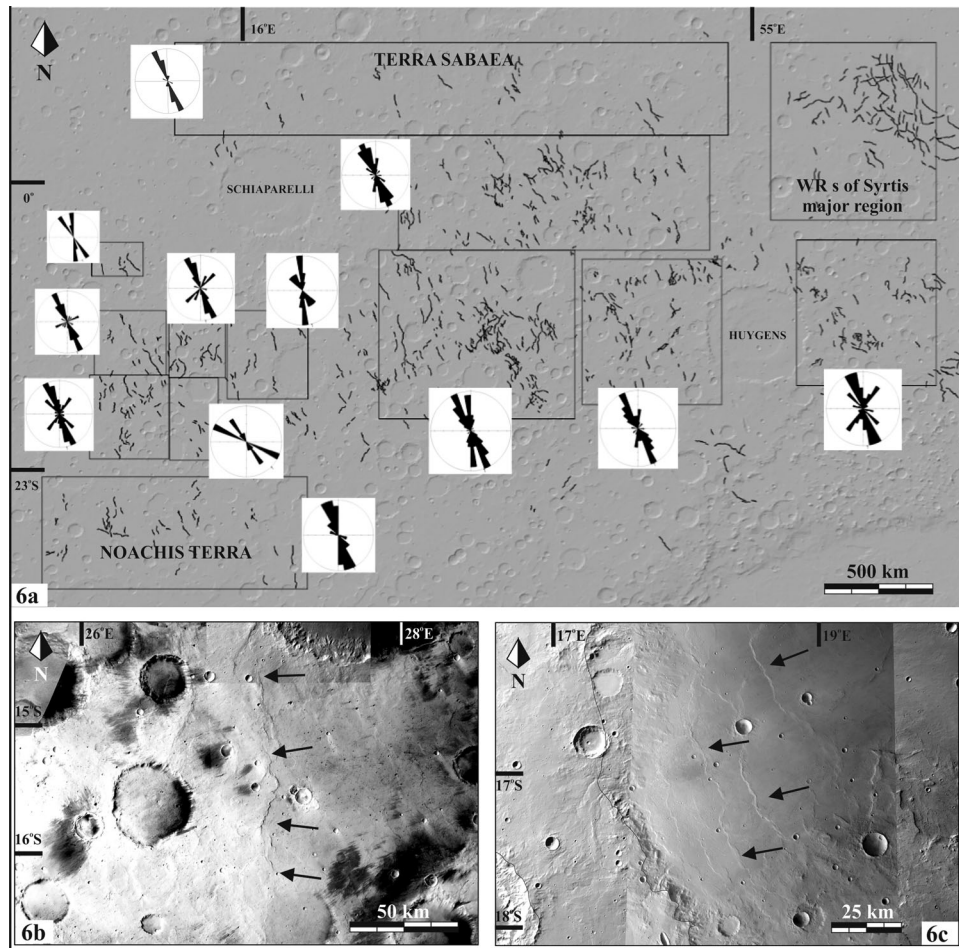


Figure 6. (a) Distribution of WR in the map region with rose diagrams representative of the WRs orientations; each rose diagram corresponds with a specific rectangular area within the map region. WRs are interpreted to be compressional structures in the deformed upper crust. WRs are shown outside (b) and inside (c) an impact crater (c).

Head, 2002). These ridges transect impact craters, thus are interpreted to have been formed during the Late Noachian or Hesperian.

5.6. Channels

Noachian channels (valley networks) (Buczowski et al., 2010; Davis et al., 2016; Hynes, Beach, & Hoke, 2010) dominate the northern part of the study area. Channels (Figure 8(a)) are interpreted to have formed during the Middle–Late Noachian; they are mostly absent in the southern part of our map region. These channels range between 5 and 20 km in width.

5.7. Lobate scarps

Lobate scarps are distributed throughout the study area. Most of the scarps are lobate in shape and interpreted to be formed by compressional stresses (Figure 8 (b)). Watters (1993) reported that lobate scarps are one sided, lobate and occur in linear or arcuate manner. The lengths of the scarp chords range up to 200 or 300 km.

5.8. Linear pit chains

These features are associated with impact cratering (Figure 8(c)). Wyrick, Ferrill, Morris, Colton, and Sims (2004) interpreted Martian pit chains to be the initial stage of graben formation. In our map region, we interpret the linear pit chains to be either formed by impact-driven radial fracturing or linear secondary impact.

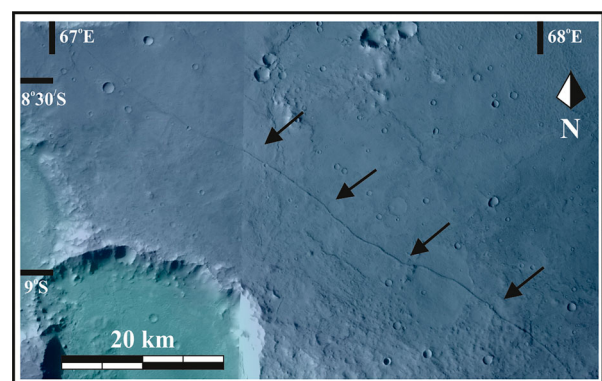


Figure 7. Linear ridge in the map region is shown using a HRSC image. These structures locate to the east of the Huygens impact basin and are interpreted to be Hesperian igneous dikes (Head et al., 2006).

Though, such features on Mars have been interpreted to mark the initial stage of graben formation (Wyrick et al., 2004).

5.9. Impact craters

5.9.1. Polygonal craters

Polygonal craters are the markers of basement structures. As has been identified on Earth, such as in the case of Meteor Crater (Shoemaker, 1959), impact crater outlines often follow earlier structural lines of weaknesses. Though, Schultz (1976) reported that the geometric shape of polygonal craters was also due to both erosion and the encroachment by lavas.

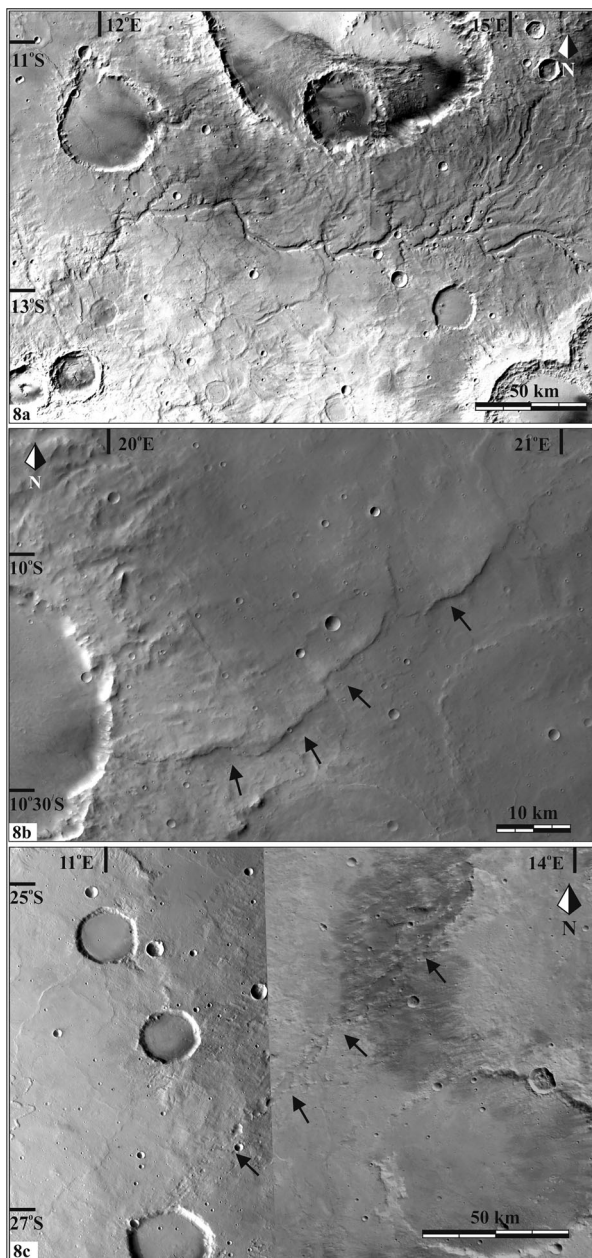


Figure 8. (a) Valley network detailed on a HRSC image. Drainage of the main channel trended from east to west during incision. (b) Lobate scarp (black arrows) is interpreted to be due to compressional tectonism in the Noachis-Sabaea region. (c) Linear pit chains (black arrows) are interpreted to have formed due to an impact-cratering event.

In the case of the Noachis-Sabaea region, the mapped polygonal craters are good indicators of pre-existing basement structures of the Martian crust, many of which are no longer visible at the surface due to both degradation and burial at the Martian surface. Polygonal craters in the study region, for example, were interpreted by Öhman et al. (2005) to indicate faults and fractures circumferential to the Hellas and Isidis impact basins. Öhman et al. (2005) classified polygonal craters into two categories: simple and complex. Simple polygonal structures of craters are interpreted to be the result of excavation flow that opens the crater, affecting the target and following the pre-existed weakness of the crust. Complex craters are interpreted to result from the modification of the crustal materials subsequent to the impact event (Eppler, Ehrlich, Nummedal, & Schultz, 1983). According to Pike (1977), larger craters tend to be polygonal more often than smaller craters.

We have mapped the polygonal craters (both simple and complex) (Figure 9(a)), as well as measured the orientations (Figure 9(b,c)) of their rims using the technique described by Öhman et al. (2005) and following Kopal (1966). Our study includes using existing map data by Öhman et al. (2005), in addition to the newly generated map data of this map investigation. We have mapped and measured more than 500 different sized polygonal craters in the map region. Our mapping investigation around the western part of the Hellas gives a better and detailed idea about the distribution of structural features and their control on the surface topography.

5.9.2. Classification of craters

We have mapped and classified the impact craters in the Noachis-Sabaea (Robbins & Hynek, 2012) region into three different types based on their age, morphology, and ejecta materials. Following Mangold et al. (2012), type 1, the oldest and largest ones with no observable ejecta, type 2, older ones with eroded ejecta and central peak, and type 3, the fresher ones with preserved ejecta and central peak. We also distinguished some as ghost craters (particularly those that can be associated with type-1 craters) (Figure 10). Of the nearly 3000 impact craters that we have investigated, 76.78% of craters are identified as type 1 (combined with ghost craters), 19.88% as type 2, and 3.34% as type 3. More or less similar percentages of crater distribution have been cited by Mangold et al. (2012) in the Arabia Terra region, north of the Noachias-Sabaea region. These classification statistics of craters clearly show an influence of the presence of the Noachian basement crust.

6. Discussion

This new morphostructural map (Main Map) depicts the tectonic elements of the Noachis-Sabaea region

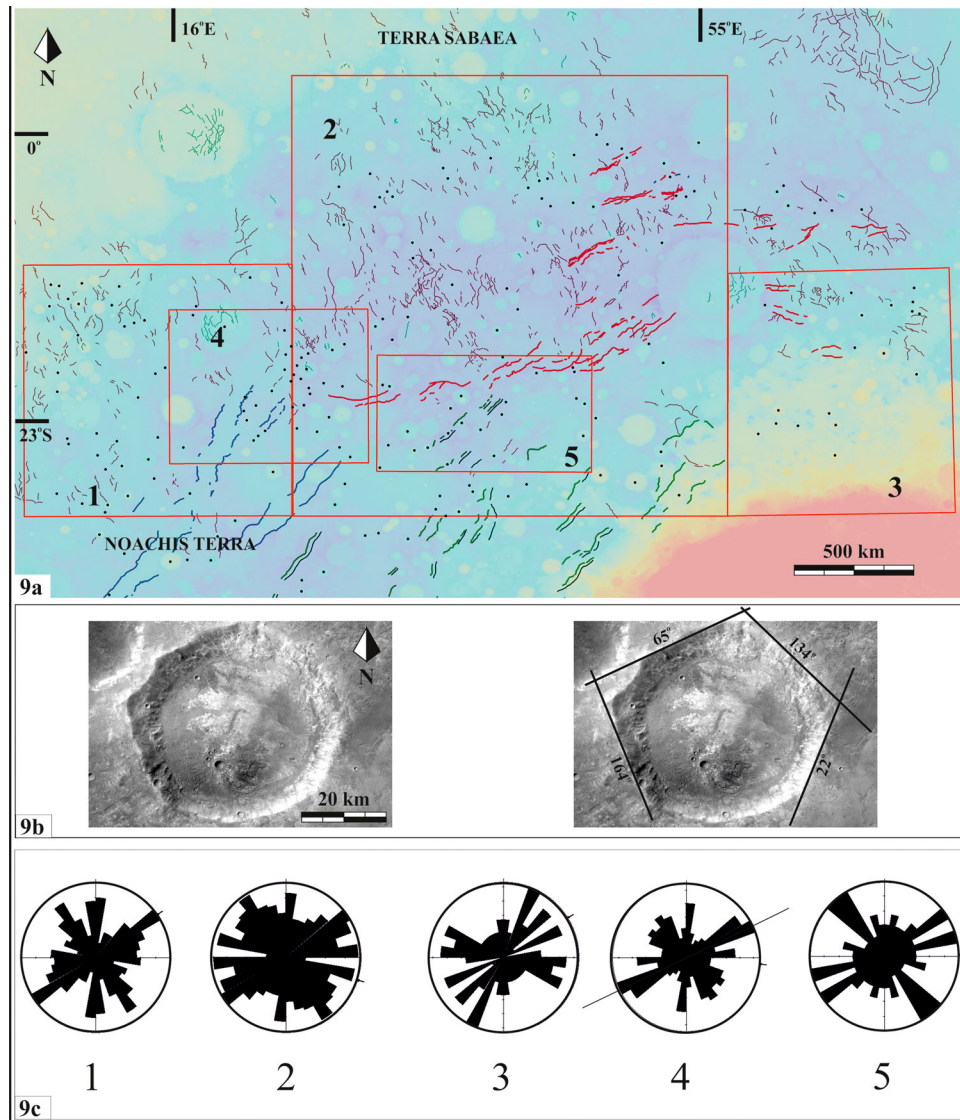


Figure 9. (a) Shown are the distribution of analysed polygonal craters (black dots marking their centres) of specific areas (red outlines and corresponding numbers) of the Noachis-Sabaea map region, along with different sets of grabens which are also shown on the geological map. (b) Polygonal crater (left) and its approximated polygonal boundaries (black lines). (c) Rose diagrams displaying the trends of the approximated boundaries of polygonal craters of specific areas (red outline) of the map region. The polygonality of the measured boundaries of the polygonal craters indicates basement structural control based on the apparent correspondence of the boundaries with the trends of graben sets. For example, two sets of faults indicated by trend appear to be associated with set-3 grabens; these grabens appear to have influenced the polygonal boundaries in rectangle 5. The boundaries of polygonal craters in rectangle 1, on the other hand, appear to be influenced by set-2 grabens. At the junction of set-2 and set-3 grabens (rectangle 4), we observe the possible influence of both sets of grabens on the formation of polygonal craters.

using the remotely sensed data. The mapped structures and their spatial relationships are subject to further study. Relative age of the structures may help to inform the evolutionary history of the region. Based on our analysis of the orientations, morphology, relative ages, and spatial and temporal relationships among the structures, as well as the rock types identified through orbital-based spectroscopy, the Noachis-Sabaea region appears to comprise structural features similar to those observed in a terrestrial tectonic zone. Using the Right Dihedral Method (placing a plane perpendicular to the plane of movement in a fault; dividing the fault into a set of 4 dihedral or quadrants), we have characterised varying directions of horizontal extension (WNW-ESE for Set-2 grabens,

NNW-SSE for Set-3 grabens), which resulted in the formation of Set-2 and Set-3 grabens. Compression, which is ENE-WSW, produced the WR on rock materials, which have been interpreted to be flood basalts (Rogers & Nazarian, 2013). The relations of the stresses and their relative timing of formation have been described by Ruj, Komatsu, Dohm, Miyamoto, and Salese (2016). In addition, the orientations of the Set-2 grabens are parallel to the ‘great faults’ identified in Terra Meridiani by Connerney et al. (2005) based on the offset of the magnetic field contours.

The topography (Smith et al., 1999) and the structures on Mars have been considered to be reshaped by internal processes, including possible plate

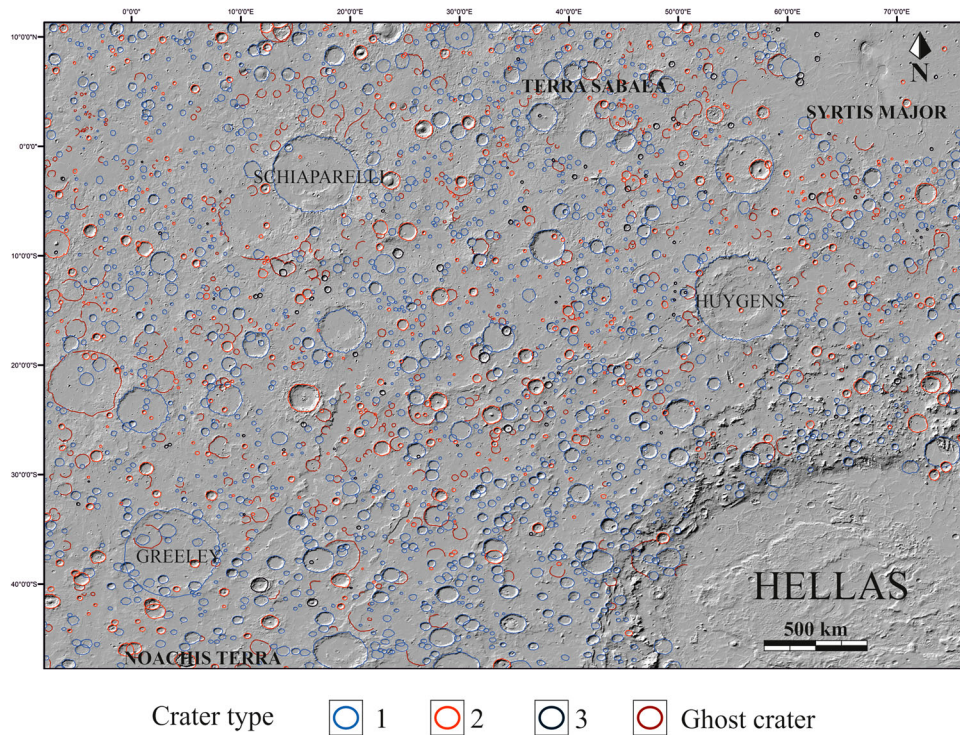


Figure 10. MOLA shaded relief map showing the distribution of different types of mapped impact craters in part based on the description by Mangold et al. (2012), which include Type-1 (blue outlines; no visible ejecta, larger in size, absence of central peak, visible fluvial landform, and estimated age >3.7 Ga), type-2 (red outlines; partially visible ejecta and fluvial landform) craters, type-3 (black outlines; absence of fluvial landform and preserved ejecta), and ghost (brown outlines; curvilinear features such as scarps of possible impact origin) craters are marked with brown outlines.

tectonics (Baker et al., 2007; Breuer & Spohn, 2003; Dohm et al., 2002, 2015; Fairén & Dohm, 2004; Maruyama, Dohm, & Baker, 2001 and references therein), surface geological processes, and impact effect of the craters. Our mappings of the morphostructures of the Noachis-Sabaea region indicate both impact and endogenic-derived activity, including an ancient mobile lithosphere that may have involved some form of plate tectonics. Further detailed geological investigation of the Noachis-Sabaea region and other ancient terrains of the southern highlands have thus the significant potential to continue to inform on the early evolution (Hadean-Archean age-equivalent) of Mars.

Software

All data were geo-referenced and then placed into an ArcGIS (ArcGIS 10.2) platform for mapping. Figures were prepared in CorelDRAW X7.

We also used stratigraphic information from the digital global geological map of Mars (Tanaka et al., 2014) to compare with the mapped tectonic structures of this morphostructural mapping investigation.

Acknowledgements

The authors sincerely thank our reviewers, Drs Antonio Funedda, Andre Pires Negrao, Douglas Howard, and

Domenico Capolongo for their detailed reviews of the map and associated text. The authors also appreciate Dr Heike Apps for quality control of the map.

Disclosure statement

No potential conflict of interest was reported by the authors.

Funding

This work was conducted as a part of PhD thesis work by T. R. supported by Università degli Studi G. d'Annunzio Chieti Pescara. J. M. D. was partially supported by JSPS KAKENHI (Grant-in-Aid for Scientific Research on Innovative Areas). Grant Number 26106002 (Hadean BioScience).

ORCID

Trishit Ruj <http://orcid.org/0000-0002-7953-4085>

Goro Komatsu <http://orcid.org/0000-0003-4155-108X>

Francesco Salese <http://orcid.org/0000-0003-0491-0274>

References

- Anderson, E. M. (1951). The dynamics of faulting. *Transactions of the Edinburgh Geological Society*, 8(3), 387–402. doi:10.1144/transed.8.3.387
- Anderson, R. C., Dohm, J. M., Golombek, M. P., Haldemann, A. F., Franklin, B. J., Tanaka, K. L., ... Peer, B. (2001). Primary centers and secondary concentrations of tectonic activity through time in the western hemisphere of Mars.

- Journal of Geophysical Research: Planets*, 106(E9), 20563–20585. doi:10.1029/2000JE001278
- Anderson, R. C., Dohm, J. M., Haldemann, A. F. C., Pouders, E., Golombek, M., & Castano, A. (2008). Centers of tectonic activity in the eastern hemisphere of Mars. *Icarus*, 195(2), 537–546. doi:10.1016/j.icarus.2007.12.027
- Anguita, F., Anguita, J., Castilla, G., De La Casa, M. A., Domínguez, J. M., Herrera, R., & Martínez, V. (1997). Arabia terra, Mars: Tectonic and palaeoclimatic evolution of a remarkable sector of Martian lithosphere. *Earth, Moon, and Planets*, 77(1), 55–72. doi:10.1023/A:1006143106970
- Anguita, F., Farelo, A. F., López, V., Mas, C., Muñoz-Espadas, M. J., Márquez, A., & Ruiz, J. (2001). Tharsis dome, Mars: New evidence for Noachian-Hesperian thick-skin and Amazonian thin-skin tectonics. *Journal of Geophysical Research: Planets*, 106(E4), 7577–7589. doi:10.1029/2000JE001246
- Ansan, V., Loizeau, D., Mangold, N., Le Mouélic, S., Carter, J., Poulet, F., ... Gondet, B. (2011). Stratigraphy, mineralogy, and origin of layered deposits inside Terby crater, Mars. *Icarus*, 211(1), 273–304. doi:10.1016/j.icarus.2010.09.011
- Baker, V. R., Maruyama, S., & Dohm, J. M. (2007). Tharsis superplume and the geological evolution of early Mars. In *Superplumes: Beyond plate tectonics* (pp. 507–522). Springer. doi:10.1007/978-1-4020-5750-2_16
- Banerdt, W. B., Golombek, M. P., & Tanaka, K. L. (1992). Stress and tectonics on Mars. *Mars*, 1, 249–297.
- Breuer, D., & Spohn, T. (2003). Early plate tectonics versus single-plate tectonics on Mars: Evidence from magnetic field history and crust evolution. *Journal of Geophysical Research*, 108(E7), 5072. doi:10.1029/2002JE001999
- Buczkowski, D. L., Seelos, K. D., Murchie, S., Seelos, F., Malaret, E., Hash, C., & CRISM Team. (2010). *Extensive phyllosilicate-bearing layer exposed by valley systems in Northwest Noachis Terra*. Lunar and planetary science conference 41, The Woodlands, Texas, p. 1458.
- Carr, M. H. (1981). *The surface of mars*. New Haven, CT: Yale University Press.
- Carr, M. H., & Head, J. W. (2010). Geologic history of Mars. *Earth and Planetary Science Letters*, 294(3), 185–203. doi:10.1016/j.epsl.2009.06.042
- Connerney, J. E. P., Acuña, M. H., Ness, N. F., Kletetschka, G., Mitchell, D. L., Lin, R. P., & Reme, H. (2005). Tectonic implications of Mars crustal magnetism. *Proceedings of the National Academy of Sciences*, 102(42), 14970–14975. doi:10.1073/pnas.0507469102
- Connerney, J. E. P., Acuna, M. H., Wasilewski, P. J., Ness, N. F., Reme, H., Mazelle, C., ... Cloutier, P. A. (1999). Magnetic lineations in the ancient crust of Mars. *Science*, 284(5415), 794–798. doi:10.1126/science.284.5415.794
- Crown, D. A., & Greeley, R. (1993). Volcanic geology of Hardriaca Patera and the eastern Hellas region of Mars. *Journal of Geophysical Research: Planets*, 98, 3431–3451. doi:10.1029/92JE02804
- Davis, J. M., Balme, M., Grindrod, P. M., Williams, R. M. E., & Gupta, S. (2016). Extensive Noachian fluvial systems in Arabia Terra: Implications for early Martian climate. *Geology*, 44(10), 847–850. doi:10.1130/G38247.1
- Davis, P. A., Tanaka, K. L., & Golombek, M. P. (1995). Topography of closed depressions, scarps, and grabens in the north Tharsis region of Mars: Implications for shallow crustal discontinuities and graben formation. *Icarus*, 114(2), 403–422. doi:10.1006/icar.1995.1071
- Dohm, J. M., Anderson, R. C., Baker, V. R., Miyamoto, H., Williams, J. P., Komatsu, G., ... Maruyama, S. (2016, March). *Non-unique systems of features on Mars and earth: Possible telltale signatures of ancient dynamic lithospheric mobility including plate tectonism*. Lunar and planetary science conference 47, The Woodlands, Texas, Abstract #2135.
- Dohm, J. M., Barlow, N. G., Anderson, R. C., Williams, J. P., Miyamoto, H., Ferris, J. C., ... Boynton, W. V. (2007). Possible ancient giant basin and related water enrichment in the Arabia terra province, Mars. *Icarus*, 190(1), 74–92. doi:10.1016/j.icarus.2007.03.006
- Dohm, J. M., Ferris, J. C., Baker, V. R., Anderson, R. C., Hare, T. M., Strom, R. G., ... Scott, D. H. (2001a). Ancient drainage basin of the Tharsis region, Mars: Potential source for outflow channel systems and putative oceans or paleolakes. *Geophysical Research: Planets*, 106, 32942–32958. doi:10.1029/2000JE001468
- Dohm, J. M., Maruyama, S., Baker, V. R., Anderson, R. C., Ferris, J. C., & Hare, T. M. (2002, March). *Plate tectonism on early Mars: Diverse geological and geophysical evidence*. Lunar and planetary science conference 33, The Woodlands, Texas, p. 1639.
- Dohm, J. M., Spagnuolo, M., Miyamoto, H., Baker, V. R., Fairen, A., Mahaney, W. C., ... Maruyama, S. (2015, March). *The Mars plate-tectonic-basement hypothesis*. Lunar and planetary science conference 46, The Woodlands, Texas, Abstract #1741 (CD-ROM).
- Eppler, D. T., Ehrlich, R., Nummedal, D., & Schultz, P. H. (1983). Sources of shape variation in lunar impact craters: Fourier shape analysis. *Geological Society of America Bulletin*, 94(2), 274–291. doi:10.1130/0016-7606(1983)94<274:SOSVIL>2.0.CO;2
- Fairén, A. G., & Dohm, J. M. (2004). Age and origin of the lowlands of Mars. *Icarus*, 168(2), 277–284. doi:10.1016/j.icarus.2003.11.025
- Fairén, A. G., Dohm, J. M., Baker, V. R., de Pablo, M. A., Ruiz, J., Ferris, J. C., & Anderson, R. C. (2003). Episodic flood inundations of the northern plains of Mars. *Icarus*, 165(1), 53–67. doi:10.1016/S0019-1035(03)00144-1
- Fairén, A. G., Ruiz, J., & Anguita, F. (2002). An origin for the linear magnetic anomalies on Mars through accretion of terranes: Implications for dynamo timing. *Icarus*, 160, 220–223. doi:10.1006/icar.2002.6942
- Frey, H., & Schultz, R. A. (1988). Large impact basins and the mega-impact origin for the crustal dichotomy on Mars. *Geophysical Research Letters*, 15(3), 229–232. doi:10.1029/GL015i003p00229
- Greeley, R., & Guest, J. (1987). *Geologic map of the eastern equatorial region of Mars*. Denver, CO: US Geological Survey.
- Head, J. W., Kreslavsky, M. A., & Pratt, S. (2002). Northern lowlands of Mars: Evidence for widespread volcanic flooding and tectonic deformation in the Hesperian period. *Journal of Geophysical Research: Planets*, 107(E1). doi:10.1029/2000JE001445
- Head, J. W., Wilson, L., Dickson, J., & Neukum, G. (2006). The Huygens-Hellas giant dike system on Mars: Implications for late Noachian-early Hesperian volcanic resurfacing and climatic evolution. *Geology*, 34(4), 285–288. doi:10.1130/G22163.1
- Hynek, B. M., Beach, M., & Hoke, M. R. (2010). Updated global map of Martian valley networks and implications for climate and hydrologic processes. *Journal of Geophysical Research: Planets*, 115(E9). doi:10.1029/2009JE003548

- Jaumann, R., Neukum, G., Behnke, T., Duxbury, T. C., Eichertopf, K., Flohrer, J., ... Hoffmann, H. (2007). The high-resolution stereo camera (HRSC) experiment on Mars express: Instrument aspects and experiment conduct from interplanetary cruise through the nominal mission. *Planetary and Space Science*, 55(7), 928–952. doi:10.1016/j.pss.2006.12.003
- Komatsu, G., Dohm, J. M., & Hare, T. M. (2004). Hydrogeologic processes of large-scale tectonomagmatic complexes in Mongolia-southern Siberia and on Mars. *Geology*, 32, 325–328. doi:10.1130/G20237.2
- Kopal, Z. (1966). *An introduction to the study of moon*. Dordrecht: Astrophysics and Space Science Library.
- Leonard, G. J., & Tanaka, K. L. (2001). *Geologic map of the Hellas region of Mars: U.S. Geological Survey Geologic Investigations Series I-2694*, pamphlet 10 p., 1 plate, scale 1:4,336,000. Retrieved from <http://pubs.usgs.gov/imap/i2694/>
- Lowry, A. R., & Zhong, S. (2003). Surface versus internal loading of the Tharsis rise, Mars. *Journal of Geophysical Research: Planets*, 108(E9). doi:10.1029/2003JE002111
- Malin, M. C., Bell, J. F., Cantor, B. A., Caplinger, M. A., Calvin, W. M., Clancy, R. T., & Lee, S. W. (2007). Context camera investigation on board the Mars reconnaissance orbiter. *Journal of Geophysical Research: Planets*, 112(E5). doi:10.1029/2006JE002808
- Mangold, N., Adeli, S., Conway, S., Ansan, V., & Langlais, B. (2012). A chronology of early Mars climatic evolution from impact crater degradation. *Journal of Geophysical Research: Planets*, 117(E4). doi:10.1029/2011JE004005
- Mangold, N., Allemand, P., & Thomas, P. G. (1998). Wrinkle ridges of Mars: Structural analysis and evidence for shallow deformation controlled by ice-rich décollements. *Planetary and Space Science*, 46(4), 345–356. doi:10.1016/S0032-0633(97)00195-5
- Maruyama, S., Dohm, J., & Baker, V. (2001, December). *Mars plate tectonics (1): An earth prospective*. AGU fall meeting abstracts, San Francisco, California, p. 0565.
- Melosh, H. J. (1976, April). *On the origin of fractures radial to lunar basins*. Lunar and planetary science conference proceedings 7, The Woodlands, Texas, pp. 2967–2982.
- Melosh, H. J., & McKinnon, W. B. (1978). The mechanics of ringed basin formation. *Geophysical Research Letters*, 5 (11), 985–988. doi:10.1029/GL005i011p00985
- Mège, D., & Masson, P. (1996). A plume tectonics model for the Tharsis province, Mars. *Planetary and Space Science*, 44(12), 1499–1546. doi:10.1016/S0032-0633(96)00113-4
- Mumma, M. J., Villanueva, G. L., Novak, R. E., Hewagama, T., Bonev, B. P., DiSanti, M. A., ... Smith, M. D. (2009). Strong release of methane on Mars in northern summer 2003. *Science*, 323(5917), 1041–1045. doi:10.1126/science.1165243
- Neukum, G., & Jaumann, R. (2004, August). HRSC: The high resolution stereo camera of Mars express. *Mars Express: The Scientific Payload*, 1240, 17–35.
- Öhman, T., Aittola, M., Kostama, V. P., & Raitala, J. (2005). The preliminary analysis of polygonal impact craters within greater Hellas region, Mars. In *Impact tectonics* (pp. 131–160). Berlin: Springer. doi:10.1007/3-540-27548-7_5
- Ormö, J., & Komatsu, G. (2003). Mars orbiter camera observation of linear and curvilinear features in the Hellas basin: Indication for multiple processes of formation. *Journal of Geophysical Research*, 108(E6), 5059. doi:10.1029/2002JE001980
- Peterson, J. E. (1977). *Geologic map of the Noachis quadrangle of Mars* (U.S. Geological Survey No. 910).
- Pike, R. J. (1977). *Apparent depth/apparent diameter relation for lunar craters*. Lunar and planetary science conference proceedings 8, The Woodlands, Texas, pp. 3427–3436.
- Robbins, S. J., & Hynek, B. M. (2012). A new global database of Mars impact craters ≥ 1 km: 1. Database creation, properties, and parameters. *Journal of Geophysical Research: Planets*, 117(E5). doi:10.1029/2011JE003966
- Rogers, A. D., Bandfield, J. L., & Christensen, P. R. (2007). Global spectral classification of Martian low-albedo regions with Mars Global Surveyor Thermal Emission Spectrometer (MGS-TES) data. *Journal of Geophysical Research: Planets*, 112(E2). doi:10.1029/2006JE002727
- Rogers, A. D., & Nazarian, A. H. (2013). Evidence for Noachian flood volcanism in Noachis Terra, Mars, and the possible role of Hellas impact basin tectonics. *Journal of Geophysical Research: Planets*, 118(5), 1094–1113. doi:10.1002/jgre.20083
- Ruff, S. W., & Christensen, P. R. (2002). Bright and dark regions on Mars: Particle size and mineralogical characteristics based on thermal emission spectrometer data. *Journal of Geophysical Research: Planets*, 107(E12). doi:10.1029/2001JE001580
- Ruj, T., Komatsu, G., Dohm, J. M., Miyamoto, H., & Salese, F. (2015). *Paleotectonism in the Noachis-Sabaea region, southern highlands of Mars; Preliminary modelling and reconstruction of events* (id. EPSC2015-255, vol. 10, p. 255). Retrieved from <http://meetingorganizer.copernicus.org/EPSC2015>
- Ruj, T., Komatsu, G., Dohm, J. M., Miyamoto, H., & Salese, F. (2016). *Effect of the Hellas impact on regional tectonism: A case study from the Noachis-Sabaea region, southern highlands of Mars*. Lunar and planetary science conference 47, The Woodlands, Texas, Abstract # 1512.
- Salese, F., Ansan, V., Mangold, N., Carter, J., Ody, A., Poulet, F., & Ori, G. G. (2016). A sedimentary origin for intercrater plains north of the Hellas basin: Implications for climate conditions and erosion rates on early Mars. *Journal of Geophysical Research: Planets*, 121. doi:10.1002/2016JE005039
- Schultz, P. H. (1976). Floor-fractured lunar craters. *The Moon*, 15(3–4), 241–273. doi:10.1007/BF00562240
- Scott, D. H., & Carr, M. H. (1978). *Geologic map of Mars map 1-1083*. Reston, VA: US Geological Survey.
- Shoemaker, E. M. (1959). *Impact mechanics at Meteor crater, Arizona* (No. 59-108). US Geological Survey.
- Sleep, N. H. (1994). Martian plate tectonics. *Journal of Geophysical Research*, 99(E3), 5639–5655. doi:10.1029/94JE00216
- Smith, D. E., Zuber, M. T., Solomon, S. C., Phillips, R. J., Head, J. W., Garvin, J. B., & Lemoine, F. G. (1999). The global topography of Mars and implications for surface evolution. *Science*, 284(5419), 1495–1503. doi:10.1126/science.284.5419.1495
- Tanaka, K. L., & Leonard, G. J. (1995). Geology and landscape evolution of the Hellas region of Mars. *Journal of Geophysical Research*, 100(E3), 5407–5432. doi:10.1029/94JE02804
- Tanaka, K. L., Robbins, S. J., Fortezzo, C. M., Skinner, J. A., & Hare, T. M. (2014). The digital global geologic map of Mars: Chronostratigraphic ages, topographic and crater morphologic characteristics, and updated resurfacing history. *Planetary and Space Science*, 95, 11–24. doi:10.1016/j.pss.2013.03.006

- Tanaka, K. L., Skinner, J. A., & Hare, T. M. (2009). *Planetary geologic mapping handbook-2009*. Retrieved from <https://ntrs.nasa.gov/search.jsp?R=20100017213>
- Watters, T. R. (1993). Compressional tectonism on Mars. *Journal of Geophysical Research*, 98(E9), 17049–17060. doi:10.1029/93JE01138
- Wichman, R. W., & Schultz, P. H. (1989). Sequence and mechanisms of deformation around the Hellas and Isidis impact basins on Mars. *Journal of Geophysical Research*, 94(B 12), 17333–17357. doi:10.1029/JB094iB12p17333
- Wilhelms, D. E., & Squyres, S. W. (1984). The Martian hemispheric dichotomy may be due to a giant impact. *Nature*, 309, 138–140. doi:10.1038/309138a0
- Wilson, L., & Head, J. W. (2002). Tharsis-radial graben systems as the surface manifestation of plume-related dike intrusion complexes: Models and implications. *Journal of Geophysical Research: Planets*, 107(E8). doi:10.1029/2001JE001593
- Wray, J. J., Hansen, S. T., Dufek, J., Swayze, G. A., Murchie, S. L., Seelos, F. P., ... Ghorso, M. S. (2013). Prolonged magmatic activity on Mars inferred from the detection of felsic rocks. *Nature Geoscience*, 6(12), 1013–1017. doi:10.1038/ngeo1994
- Wyrick, D., Ferrill, D. A., Morris, A. P., Colton, S. L., & Sims, D. W. (2004). Distribution, morphology, and origins of Martian pit crater chains. *Journal of Geophysical Research: Planets*, 109(E6). doi:10.1029/2004JE002240
- Yin, A. (2012). Structural analysis of the Valles Marineris fault zone: Possible evidence for large-scale strike-slip faulting on Mars. *Lithosphere*, 4(4), 286–330. doi:10.1130/L192.1